

Fig. 3. ORTEP drawing of the TCM ligand with 50% probability ellipsoids for the RT determination of compound (1).

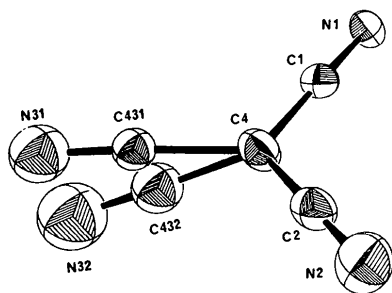


Fig. 4. ORTEP drawing of TCM with 50% probability ellipsoids for the LT determination of compound (1).

These studies are supported by the National Science Council (NSC81-0208-M031-03) of the Republic of China on Taiwan.

#### References

- BAUKOVA, T. V., KRAVTSOV, D. N., KUZ'MINA, L. G., DVORTSOVA, N. V., PORAY-KOSHITS, M. A. & PEREVALOVA, E. G. (1989). *J. Organomet. Chem.* **372**, 465–471.
- BIONDI, C., BONAMICO, M., TORELLI, L. & VACIAGE, A. (1965). *Chem. Commun.* **10**, 191–192.
- BRITTON, D. & CHOW, Y. M. (1983). *Acta Cryst.* **C39**, 1539–1540.
- CHOW, Y. M. & BRITTON, D. (1975). *Acta Cryst.* **B31**, 1934–1937.
- FRENZ, B. A. (1989). *Personal SDP – a Real-Time System for Solving, Refining and Displaying Crystal Structures*. College Station, Texas, USA.
- JOHNSON, C. K. (1970). *ORTEP*. Report ORNL-3794, 2nd revision. Oak Ridge National Laboratory, Tennessee, USA.
- KONNERT, J. & BRITTON, D. (1966). *Inorg. Chem.* **5**, 1193–1196.
- LENARDA, M. & BADDLEY, W. H. (1972). *J. Organomet. Chem.* **39**, 217–224.
- SHELDRICK, G. M. (1976). *SHELX76*. Program for crystal structure determination. Univ. of Cambridge, England.
- SUMMERVILLE, D. A., COHEN, I. A., HATANO, K. & SCHEIDT, W. R. (1978). *Inorg. Chem.* **17**, 2906–2910.
- WANG, J. C. (1987). PhD thesis, Louisiana State Univ., Baton Rouge, Louisiana, USA.
- WITT, M. E. (1973). PhD thesis, Louisiana State Univ., Baton Rouge, Louisiana, USA.

*Acta Cryst.* (1993). **B49**, 685–691

## Structures at 293 and 100 K of $\beta$ -Tetrakis[bis(ethylenedithio)tetrathiafulvalene] Tetracyanonickelate(II): $\beta$ -[BEDT-TTF]<sub>4</sub>[Ni(CN)<sub>4</sub>]

BY MOHAMMED FETTOUHI, LAHCÈNE OUAHAB\* AND DANIEL GRANDJEAN

*Laboratoire de Chimie du Solide et Inorganique Moléculaire, URA 254, CNRS, Université de Rennes I, 35042 Rennes CEDEX, France*

AND LOÏC TOUPET

*Groupe Matière Condensée et matériaux, URA 804, CNRS, Université de Rennes I, 35042 Rennes CEDEX, France*

(Received 15 March 1992; accepted 1 October 1992)

#### Abstract

[C<sub>10</sub>H<sub>8</sub>S<sub>8</sub>]<sub>4</sub>[Ni(CN)<sub>4</sub>],  $M_r = 1701.53$ ,  $F(000) = 864$ ,  $\lambda(\text{Mo K}\alpha) = 0.71073 \text{ \AA}$ . At 293 K: triclinic,  $P\bar{1}$ ,  $a = 9.677(7)$ ,  $b = 10.960(6)$ ,  $c = 16.392(8) \text{ \AA}$ ,  $\alpha = 95.95(5)$ ,  $\beta = 97.85(5)$ ,  $\gamma = 115.13(5)^\circ$ ,  $V = 1533(4) \text{ \AA}^3$ ,  $Z = 1$ ,  $D_x = 1.842 \text{ g cm}^{-3}$ ,  $\mu = 14.06 \text{ cm}^{-1}$ ,  $R = 0.031$  based on 3565 observed reflections with  $I \geq 6\sigma(I)$ . At 100 K: triclinic,  $P\bar{1}$ ,  $a = 9.721(4)$ ,  $b = 10.761(4)$ ,  $c = 16.431(5) \text{ \AA}$ ,  $\alpha =$

$95.87(3)$ ,  $\beta = 98.17(4)$ ,  $\lambda = 115.71(3)^\circ$ ,  $V = 1507(2) \text{ \AA}^3$ ,  $Z = 1$ ,  $D_x = 1.875 \text{ g cm}^{-3}$ ,  $\mu = 14.31 \text{ cm}^{-1}$ ,  $R = 0.082$  based on 3865 observed reflections with  $I \geq 6\sigma(I)$ . The C atoms of the terminal ethylenic groups of each independent BEDT-TTF molecule are statistically distributed on both sides of the molecular mean plane at room temperature. This phenomenon disappears at 100 K where the BEDT-TTF molecules adopt different conformations. The organic molecules develop tetramerized stacks along the [210] direction. The structure belongs to the  $\beta$  type of the BEDT-TTF series.

\* Author to whom correspondence should be addressed.

### Introduction

We recently reported the structures and properties of some new organic conducting salts made of tetrathiafulvalene (TTF) derivatives and planar tetracyanometalate dianions (Ouahab, Padiou, Grandjean, Garrigou-Lagrange, Delhaes & Bencharif, 1989; Ouahab, Triki, Grandjean, Bencharif, Garrigou-Lagrange & Delhaes, 1990; Garrigou-Lagrange, Ouahab, Grandjean & Delhaes, 1990). The two  $\beta$ -[BEDT-TTF]<sub>4</sub>[M(CN)<sub>4</sub>] [BEDT-TTF or ET = bis(ethylenedithiotetrathiafulvalene), M = Pt<sup>II</sup>, Ni<sup>II</sup>] salts exhibit metallic behaviour down to 250 K where a broad metal-insulator transition occurs. In order to understand the nature of this transition we have determined the X-ray crystal structures for both platinate and nickelate salts at room temperature and at low temperature. Recently, we reported the complete study of the platinate salt (Fettouhi, Ouahab, Grandjean & Toupet, 1992). Since then, the X-ray crystal structure of the nickelate salt at room temperature has been reported (Kawamoto, Tanaka & Tanaka, 1991). We report here the room-temperature crystal structure with more details on the statistical disorder of the terminal ethylenic groups of the ET molecules, the structure at 100 K and the temperature dependence of the unit-cell parameters of the nickelate salt:  $\beta$ -[BEDT-TTF]<sub>4</sub>[Ni(CN)<sub>4</sub>].

### Experimental

The title compound was deposited on a platinum-wire electrode by anodic oxidation of the organic donor ( $4 \times 10^{-3}$  M) under low constant current ( $I = 1 \mu\text{A}$ ) in the presence of the dianion tetraethylammonium salt ( $10^{-2}$  M) as supporting electrolyte. The crystal growth solvent is a mixture of DMF (dimethylformamide) and CH<sub>2</sub>Cl<sub>2</sub> (ratio 4:1). The stoichiometries were determined by X-ray crystal structure analysis.

The X-ray crystal structures were solved at room temperature and 100 K using two different single crystals and using an Enraf-Nonius CAD-4 diffractometer equipped with graphite-monochromatized Mo K $\alpha$  ( $\lambda = 0.71073 \text{ \AA}$ ) radiation. The unit-cell parameters were determined and refined from the setting angles of 25 accurately centred reflections.

#### Room temperature

A black crystal of approximate dimensions of  $0.4 \times 0.3 \times 0.15$  mm was selected for data collection. Data were collected with  $\theta$ - $2\theta$  scans. The intensities were corrected for Lorentz and polarization effects. No absorption corrections were applied. The structure was solved by direct methods and successive Fourier difference synthesis. The refinements (on  $F$ )

were performed by the full-matrix least-squares method [H atoms, placed at computed positions ( $C-H = 1 \text{ \AA}$ ,  $B = 5 \text{ \AA}^2$ ), were not refined]. The C atoms of the ethylenic groups show statistical disorder on two sites. The refined occupancy parameters are given in Table 2(a).

#### Structure at 100 K

Crystal dimensions were  $0.5 \times 0.25 \times 0.2$  mm. The sample was cooled by a nitrogen stream. The temperatures were deduced by measuring the temperature of the nitrogen stream near the sample with a thermocouple. After the stabilization of the temperature, the unit-cell parameters were refined by least squares following a *SETANG* procedure (Enraf-Nonius, 1985). Each point was measured during the decrease and the increase of temperature. We observed complete reversibility in the measurements. Data were collected with  $\theta$ - $2\theta$  scans. The intensities were corrected for Lorentz and polarization effects. The absorption corrections were performed using the *DIFABS* procedure (Walker & Stuart, 1983) and the correction factors ranged from 0.677 to 2.001. The structure was refined starting from the atomic coordinates of the room-temperature structure except those of the terminal ethylenic groups. The latter were found by a Fourier difference synthesis. In this case, and after using different weighting schemes, the best results were obtained using a unit weight for all data.

Crystal characteristics and refinement data are summarized in Table 1. Scattering factors were taken from *International Tables for X-ray Crystallography* (1974, Vol. IV). All the calculations were performed on a MicroVAX 3100 using the *SDP* programs (B. A. Frenz & Associates Inc., 1985). The atomic coordinates are given in Tables 2(a) and 2(b). The comparative bond distances and bond angles are given in Tables 3(a) and 3(b). The atomic numbering is shown in Fig. 1.\*

### Discussion

The crystal structure represented in Fig. 2 is built up of Ni(CN)<sub>4</sub><sup>2-</sup> anions located at the origin of the lattice, and two ET molecules (denoted *A* and *B*) which stack along the [210] direction as a tetramerized [BAAB][BAAB]... sequence.

The Ni—C bond distances and bond angles compare well with those found, for instance, in the (TMTTF)<sub>2</sub>Ni(CN)<sub>4</sub> salt (Bencharif & Ouahab, 1988).

\* Lists of structure factors, anisotropic thermal parameters and H-atom coordinates have been deposited with the British Library Document Supply Centre as Supplementary Publication No. SUP 55960 (51 pp.). Copies may be obtained through The Technical Editor, International Union of Crystallography, 5 Abbey Square, Chester CH1 2HU, England. [CIF reference: PA0283]

Table 1. *Crystal, data-collection and refinement information*

	293 K	100 K
Crystal dimensions (mm)	0.4 × 0.3 × 0.15	0.5 × 0.25 × 0.2
2θ range (°)	2 to 52	2 to 50
Range of h	0 to 11	0 to 11
k	-13 to 13	-12 to 12
l	-20 to 20	-19 to 19
Standard reflections	213	037
	037	133
	313	443
Average deviation (%)	-2.5	-1.5
$\mu$ (Mo K $\alpha$ ) (cm <sup>-1</sup> )	14.06	14.31
No. of measured reflections	6098	5592
No. of unique reflections	5340	4916
R <sub>int</sub>	0.013	0.093
Reflections with I > 6σ(I)	3565	3865
No. of variables	434	363
Weighting scheme	4F <sub>i</sub> <sup>2</sup> /(σ <sup>2</sup> (I) + (0.07F <sub>i</sub> ) <sup>2</sup> )	Unit weight
R, wR	0.031, 0.046	0.082, 0.105
S	1.18	4.69
(Δ/σ) <sub>max</sub>	0.47	0.02
Δρ <sub>max</sub> , Δρ <sub>min</sub> (e Å <sup>-3</sup> )	0.394, -0.170	1.776, -1.527

Table 2. *Atomic coordinates and equivalent isotropic thermal parameters for (BEDT-TTF)<sub>4</sub>Ni(CN)<sub>4</sub> (M = multiplicity)*

	x	y	z	B <sub>eq</sub> (Å <sup>2</sup> )	M
(a) At 293 K					
Ni	0	0	0	2.67 (1)	
S1	0.40460 (8)	0.59158 (7)	0.56700 (5)	3.52 (2)	
S2	0.21029 (8)	0.73237 (7)	0.58628 (4)	3.45 (2)	
S3	0.05189 (8)	0.63256 (7)	0.39324 (5)	3.42 (2)	
S4	0.24735 (8)	0.49492 (7)	0.36835 (4)	3.35 (2)	
S5	-0.10497 (8)	0.56830 (8)	0.21812 (5)	3.94 (2)	
S6	0.13722 (8)	0.41057 (7)	0.18632 (5)	3.44 (2)	
S7	0.32577 (8)	0.83220 (7)	0.76718 (5)	3.39 (2)	
S8	0.55988 (8)	0.66433 (8)	0.74300 (5)	3.74 (2)	
S9	0.50248 (8)	0.85693 (7)	0.34021 (5)	3.60 (2)	
S10	0.67801 (8)	0.69830 (7)	0.32101 (4)	3.35 (2)	
S11	0.84821 (9)	0.80280 (8)	0.51243 (5)	3.93 (2)	
S12	0.66618 (8)	0.95459 (8)	0.53807 (5)	3.87 (2)	
S13	1.0349 (1)	0.89655 (9)	0.68293 (6)	5.95 (2)	
S14	0.81522 (9)	1.07288 (8)	0.71305 (5)	4.17 (2)	
S15	0.37183 (9)	0.80875 (8)	0.15955 (5)	3.51 (2)	
S16	0.58774 (9)	0.62478 (8)	0.13885 (5)	4.53 (2)	
N1	-0.2658 (3)	0.0644 (3)	0.0247 (2)	4.90 (8)	
N2	0.1939 (3)	0.3016 (3)	0.0085 (2)	4.14 (7)	
C1	-0.1662 (3)	0.0389 (3)	0.0142 (2)	3.16 (7)	
C2	0.1221 (3)	0.1884 (3)	0.0054 (2)	3.09 (7)	
C3	0.2628 (3)	0.6326 (3)	0.5203 (2)	2.82 (6)	
C4	0.4248 (3)	0.6758 (3)	0.6675 (2)	2.63 (6)	
C5	0.3344 (3)	0.7405 (3)	0.6763 (2)	2.52 (6)	
C6	-0.0476 (4)	0.5305 (3)	0.1235 (2)	4.21 (8)	
C7	-0.0261 (4)	0.4031 (3)	0.1151 (2)	4.22 (8)	
C8	0.1943 (3)	0.5902 (3)	0.4375 (2)	2.76 (6)	
C9	0.0321 (3)	0.5540 (3)	0.2916 (2)	2.87 (6)	
C10	0.1235 (3)	0.4922 (3)	0.2795 (2)	2.48 (6)	
C11	0.4992 (7)	0.8512 (6)	0.8350 (4)	2.2 (1)*	0.44 (6)
C11'	0.4431 (6)	0.7975 (7)	0.8470 (3)	4.3 (2)*	0.52 (7)
C12	0.5903 (7)	0.8035 (7)	0.8242 (4)	3.7 (2)*	0.48 (7)
C12'	0.5071 (6)	0.7174 (5)	0.8376 (3)	3.7 (1)*	0.55 (7)
C13	0.6366 (3)	0.8066 (3)	0.3870 (2)	2.66 (6)	
C14	0.4868 (3)	0.7784 (3)	0.2384 (2)	2.65 (6)	
C15	0.5679 (3)	0.7066 (3)	0.2299 (2)	2.70 (6)	
C16	0.9823 (6)	0.9406 (5)	0.7771 (3)	3.6 (1)*	0.52 (6)
C16'	1.0523 (9)	1.0076 (9)	0.7695 (5)	5.8 (2)*	0.48 (8)
C17	0.9258 (8)	1.0305 (8)	0.7917 (4)	5.7 (2)*	0.52 (7)
C17'	0.9832 (7)	1.0816 (6)	0.7816 (4)	2.7 (1)*	0.47 (6)
C18	0.7088 (3)	0.8499 (3)	0.4693 (2)	2.93 (6)	
C19	0.8902 (3)	0.9012 (3)	0.6106 (2)	3.21 (7)	
C20	0.8056 (3)	0.9709 (3)	0.6228 (2)	2.68 (6)	
C21	0.4581 (6)	0.7818 (5)	0.0728 (3)	3.6 (1)*	0.59 (7)
C21'	0.3629 (8)	0.6964 (7)	0.0692 (4)	2.6 (2)*	0.40 (6)
C22	0.5068 (7)	0.6891 (6)	0.0563 (4)	5.5 (2)*	0.47 (7)
C22'	0.4541 (7)	0.6419 (6)	0.0645 (3)	3.0 (1)*	0.51 (6)
(b) At 100 K					
Ni	0.000	0.000	0.000	1.27 (4)	
S1	0.4093 (3)	0.5946 (3)	0.5709 (2)	1.50 (6)	
S2	0.2133 (3)	0.7372 (3)	0.5905 (2)	1.44 (6)	

Table 2 (cont.)

	x	y	z	B <sub>eq</sub> (Å <sup>2</sup> )	M
S3	0.0486 (3)	0.6316 (3)	0.3987 (2)	1.44 (6)	
S4	0.2511 (3)	0.4987 (3)	0.3711 (2)	1.35 (6)	
S5	-0.1187 (3)	0.5566 (3)	0.2238 (2)	1.38 (6)	
S6	0.1379 (3)	0.4145 (3)	0.1890 (2)	1.43 (6)	
S7	0.3206 (3)	0.8297 (3)	0.7729 (2)	1.39 (6)	
S8	0.5552 (3)	0.6597 (3)	0.7495 (2)	1.51 (6)	
S9	0.5067 (3)	0.8652 (3)	0.3370 (2)	1.51 (6)	
S10	0.6803 (3)	0.7006 (3)	0.3184 (2)	1.40 (6)	
S11	0.8496 (3)	0.8044 (3)	0.5105 (2)	1.63 (6)	
S12	0.6681 (3)	0.9601 (3)	0.5368 (2)	1.59 (6)	
S13	1.0396 (3)	0.9019 (3)	0.6823 (2)	1.99 (7)	
S14	0.8167 (3)	1.0791 (3)	0.7127 (2)	1.59 (6)	
S15	0.3800 (3)	0.8209 (3)	0.1557 (2)	1.58 (6)	
S16	0.5918 (3)	0.6277 (3)	0.1345 (2)	1.97 (7)	
N1	-0.269 (1)	0.061 (1)	0.0219 (7)	2.2 (2)	
N2	0.195 (1)	0.315 (1)	0.0124 (6)	2.1 (2)	
C1	-0.168 (1)	0.034 (1)	0.0123 (7)	1.4 (2)†	
C2	0.122 (1)	0.192 (1)	0.0066 (7)	1.4 (3)	
C3	0.261 (1)	0.629 (1)	0.5237 (7)	1.4 (2)	
C4	0.422 (1)	0.675 (1)	0.6724 (7)	1.4 (3)	
C5	0.331 (1)	0.737 (1)	0.6814 (7)	1.0 (2)	
C6	-0.044 (1)	0.541 (1)	0.1308 (7)	1.4 (2)	
C7	-0.024 (1)	0.409 (1)	0.1156 (7)	1.3 (3)	
C8	0.195 (1)	0.591 (1)	0.4423 (7)	1.4 (2)	
C9	0.025 (1)	0.550 (1)	0.2968 (7)	1.3 (2)	
C10	0.119 (1)	0.492 (1)	0.2836 (7)	1.0 (2)	
C11	0.442 (1)	0.798 (1)	0.8543 (7)	1.8 (3)	
C12	0.588 (1)	0.799 (1)	0.8298 (7)	1.9 (3)	
C13	0.644 (1)	0.816 (1)	0.3857 (7)	1.3 (2)	
C14	0.494 (1)	0.787 (1)	0.2349 (7)	1.7 (3)	
C15	0.575 (1)	0.716 (1)	0.2263 (7)	0.9 (2)	
C16	0.984 (1)	0.943 (1)	0.7775 (7)	1.9 (3)	
C17	0.974 (1)	1.079 (2)	0.7860 (7)	2.2 (3)	
C18	0.711 (1)	0.855 (1)	0.4656 (7)	1.4 (2)	
C19	0.833 (1)	0.907 (1)	0.6091 (7)	1.8 (3)	
C20	0.810 (1)	0.973 (1)	0.6215 (7)	1.1 (2)	
C21	0.360 (1)	0.697 (1)	0.6070 (7)	1.7 (3)	
C22	0.515 (1)	0.702 (1)	0.0561 (7)	2.1 (3)	

\* Occupancy refinement performed.

† Refined isotropically.

Table 3. *Bond distances (Å) and bond angles (°) in (BEDT-TTF)<sub>4</sub>Ni(CN)<sub>4</sub>*

(a) At 293 K					
Ni—C1	1.867 (4)	S14—C17	1.786 (8)		
Ni—C2	1.879 (3)	S14—C17'	1.805 (6)		
S1—C3	1.726 (3)	S14—C20	1.726 (3)		
S1—C4	1.746 (3)	S15—C14	1.741 (3)		
S2—C3	1.733 (3)	S15—C21	1.803 (6)		
S2—C5	1.740 (3)	S15—C21'	1.792 (8)		
S3—C8	1.727 (3)	S16—C15	1.737 (3)		
S3—C9	1.740 (3)	S16—C22	1.822 (8)		
S4—C8	1.734 (3)	S16—C22'	1.736 (6)		
S4—C10	1.744 (3)	N1—C1	1.142 (5)		
S5—C6	1.784 (4)	N2—C2	1.127 (4)		
S5—C9	1.736 (3)	C3—C8	1.363 (4)		
S6—C7	1.798 (4)	C4—C5	1.352 (5)		
S6—C10	1.739 (3)	C6—C7	1.492 (6)		
S7—C5	1.741 (3)	C9—C10	1.345 (5)		
S7—C11	1.800 (6)	C11—C12	1.22 (1)		
S7—C11'	1.792 (7)	C11—C12'	1.51 (1)		
S8—C4	1.727 (3)	C11'—C12	1.50 (1)		
S8—C12	1.809 (7)	C11'—C12'	1.28 (1)		
S8—C13	1.813 (6)	C13—C18	1.364 (4)		
S9—C13	1.732 (3)	C14—C15	1.336 (5)		
S9—C14	1.752 (3)	C16—C17	1.33 (1)		
S10—C13	1.731 (3)	C16—C17'	1.535 (9)		
S10—C15	1.746 (3)	C16'—C17	1.43 (1)		
S11—C18	1.730 (4)	C16'—C17'	1.27 (1)		
S11—C19	1.735 (3)	C19—C20	1.355 (5)		
S12—C18	1.737 (3)	C21—C22	1.31 (1)		
S12—C20	1.735 (3)	C21—C22'	1.508 (9)		
S13—C16	1.773 (6)	C21'—C22	1.47 (1)		
S13—C16'	1.710 (9)	C21'—C22'	1.26 (1)		
S13—C19	1.729 (3)				
C1—Ni—C2	88.0 (1)	S1—C4—C5	116.7 (2)	S15—C14—C15	127.6 (2)
C3—S1—C4	95.5 (2)	S8—C4—C5	128.7 (2)	S10—C15—S16	113.8 (2)
C3—S2—C5	95.6 (1)	S2—C5—S7	115.0 (2)	S10—C15—C14	117.2 (2)

Table 3 (cont.)

C8—S3—C9	95.5 (2)	S2—C5—C4	116.8 (2)	S16—C15—C14	128.9 (2)
C8—S4—C10	95.6 (1)	S7—C5—C4	128.1 (2)	S13—C16—C17	126.7 (5)
C6—S5—C9	100.8 (2)	S5—C6—C7	114.4 (2)	S13—C16—C17	110.2 (4)
C7—S6—C10	101.5 (2)	S6—C7—C6	115.4 (2)	S13—C16—C17	124.1 (5)
C5—S7—C11	99.9 (2)	S3—C8—S4	115.1 (1)	S13—C16—C17	131.0 (6)
C5—S7—C11'	102.6 (2)	S3—C8—C3	122.1 (3)	S14—C17—C16	124.5 (5)
C4—S8—C12	100.0 (3)	S4—C8—C3	122.8 (3)	S14—C17—C16'	117.1 (5)
C4—S8—C12'	100.7 (2)	S5—C9—S5	114.2 (2)	S14—C17—C16	111.6 (3)
C13—S9—C14	95.3 (1)	S3—C9—C10	117.3 (2)	S14—C17—C16'	126.4 (5)
C13—S10—C15	95.3 (2)	S5—C9—C10	128.5 (2)	S11—C18—S12	115.4 (1)
C18—S11—C19	95.2 (2)	S4—C10—S6	114.9 (2)	S11—C18—C13	122.1 (3)
C18—S12—C20	95.2 (2)	S4—C10—C9	116.4 (2)	S12—C18—C13	122.5 (3)
C16—S13—C19	99.9 (2)	S6—C10—C9	128.7 (2)	S11—C19—S13	115.5 (2)
C16—S13—C19	103.6 (4)	S7—C11—C12	130.8 (5)	S11—C19—C20	117.2 (2)
C17—S14—C20	102.9 (3)	S7—C11—C12'	113.0 (3)	S13—C19—C20	127.3 (2)
C17—S14—C20	102.2 (2)	S7—C11'—C12	113.8 (4)	S12—C20—S14	114.8 (2)
C14—S15—C21	99.1 (2)	S7—C11'—C12'	127.2 (4)	S12—C20—C19	116.8 (2)
C14—S15—C21'	102.5 (3)	S8—C12—C11	127.0 (5)	S14—C20—C19	128.4 (2)
C15—S16—C22	103.5 (3)	S8—C12—C11'	114.0 (4)	S15—C21—C22	128.3 (5)
C15—S16—C22'	101.1 (2)	S8—C12'—C11	110.2 (4)	S15—C21—C22'	110.0 (4)
Ni—C1—N1	178.4 (3)	S8—C12'—C11'	127.1 (5)	S15—C21'—C22	118.5 (4)
Ni—C2—N2	179.3 (3)	S9—C13—S10	115.2 (1)	S15—C21'—C22'	124.7 (5)
S1—C3—S2	115.3 (1)	S9—C13—C18	123.6 (3)	S16—C22—C21	122.0 (4)
S1—C3—C8	123.5 (3)	S10—C13—C18	121.2 (3)	S16—C22—C21'	113.4 (5)
S2—C3—C8	121.2 (3)	S9—C14—S15	115.6 (2)	S16—C22—C21	115.6 (3)
S1—C4—S8	114.5 (2)	S9—C14—C15	116.8 (2)	S16—C22—C21'	133.1 (5)

## (b) At 100 K

Ni—C1	1.86 (1)	S11—C18	1.76 (1)
Ni—C1	1.86 (1)	S11—C19	1.75 (1)
Ni—C2	1.87 (1)	S12—C18	1.76 (1)
Ni—C2	1.87 (1)	S12—C20	1.76 (1)
S1—C3	1.74 (1)	S13—C16	1.80 (1)
S1—C4	1.76 (1)	S13—C19	1.76 (1)
S2—C3	1.77 (1)	S14—C17	1.81 (1)
S2—C5	1.75 (1)	S14—C20	1.76 (1)
S3—C8	1.74 (1)	S15—C14	1.75 (1)
S3—C9	1.74 (1)	S15—C21	1.80 (1)
S4—C8	1.75 (1)	S16—C15	1.77 (1)
S4—C10	1.76 (1)	S16—C22	1.82 (2)
S5—C6	1.80 (1)	N1—C1	1.16 (2)
S5—C9	1.73 (1)	N2—C2	1.18 (2)
S6—C7	1.82 (1)	C3—C8	1.34 (2)
S6—C10	1.76 (1)	C4—C5	1.33 (2)
S7—C5	1.76 (1)	C6—C7	1.52 (2)
S7—C11	1.82 (1)	C9—C10	1.35 (2)
S8—C4	1.75 (1)	C11—C12	1.53 (2)
S8—C12	1.77 (1)	C13—C18	1.32 (1)
S9—C13	1.76 (1)	C14—C15	1.33 (2)
S9—C14	1.76 (1)	C16—C17	1.50 (2)
S10—C13	1.76 (1)	C19—C20	1.31 (2)
S10—C15	1.77 (1)	C21—C22	1.51 (2)

The charge on each ET molecule has been assumed to be +0.5 on the basis of the comparison (Table 4) of its geometrical parameters with those found for a variety of oxidation states of that molecule, *i.e.* ET<sup>0</sup> (Kobayashi, Kobayashi, Sasaki, Saïto & Inokuchi, 1986), ET<sup>0.5+</sup> (Mallah, Hollis, Bott, Kurmoo, Day, Allan & Friend, 1990) and ET<sup>+</sup> (Triki, Ouahab, Grandjean & Fabre, 1991), and those found in the corresponding Pt salt (Fettouhi *et al.*, 1992). In agreement with this result, the 4:1 stoichiometry of this salt suggests that the ET molecules bear a mean charge of +0.5.

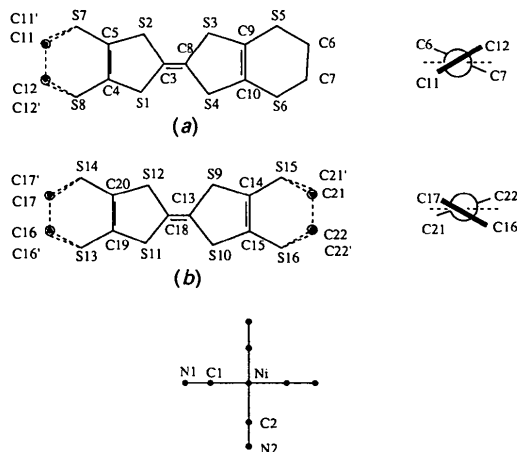


Fig. 1. Atomic numbering at both temperatures showing (a) the disordered ethylenic groups at 293 K and (b) their conformation at 100 K (the mean plane is represented by the dashed line).

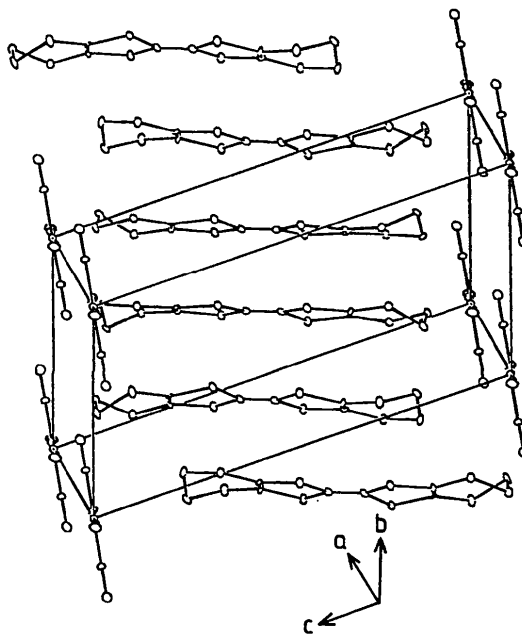


Fig. 2. Unit-cell content at 100 K.

C1—Ni—C1	180	S3—C8—S4	115.0 (6)
C1—Ni—C2	88.9 (5)	S3—C8—C3	123.0 (1)
C1—Ni—C2	91.1 (5)	S4—C8—C3	122.0 (1)
C2—Ni—C2	180	S3—C9—S5	115.2 (8)
C3—S1—C4	95.1 (6)	S3—C9—C10	117.0 (8)
C3—S2—C5	94.8 (6)	S5—C9—C10	127.8 (8)
C8—S3—C9	95.8 (6)	S4—C10—S6	113.5 (8)
C8—S4—C10	94.9 (6)	S4—C10—C9	117.3 (8)
C6—S5—C9	99.2 (6)	S6—C10—C9	129.2 (9)
C7—S6—C10	101.8 (6)	S7—C11—C12	114.0 (8)
C5—S7—C11	102.7 (6)	S8—C12—C11	115.7 (7)
C4—S8—C12	100.3 (7)	S9—C13—S10	113.9 (5)
C13—S9—C14	95.7 (6)	S9—C13—C18	125.0 (1)
C13—S10—C15	94.9 (6)	S10—C13—C18	121.0 (1)
C18—S11—C19	94.9 (7)	S9—C14—S15	114.9 (9)
C18—S12—C20	94.5 (6)	S9—C14—C15	117.2 (9)
C16—S13—C19	99.7 (6)	S15—C14—C15	127.9 (9)
C17—S14—C20	102.2 (7)	S10—C15—S16	113.0 (8)
C14—S15—C21	101.5 (7)	S10—C15—C14	117.5 (8)
C15—S16—C22	100.0 (6)	S16—C15—C14	129.5 (9)
Ni—C1—N1	177.2 (9)	S13—C16—C17	113.3 (9)
Ni—C2—N2	177.0 (1)	S14—C17—C16	115.0 (7)
S1—C3—S2	114.5 (6)	S11—C18—S12	114.3 (6)
S1—C3—C8	125.0 (1)	S11—C18—C13	123.0 (1)
S2—C3—C8	120.0 (1)	S12—C18—C13	123.0 (1)
S1—C4—S8	113.8 (8)	S11—C19—S13	115 (1)
S1—C4—C5	117.7 (9)	S11—C19—C20	117.9 (9)
S8—C4—C5	128.5 (9)	S13—C19—C20	127.5 (9)
S2—C5—S7	113.8 (8)	S12—C20—S14	112.2 (8)
S2—C5—C4	117.2 (8)	S12—C20—C19	118.1 (8)
S7—C5—C4	128.8 (8)	S14—C20—C19	129.7 (9)
S5—C6—C7	113.1 (8)	S15—C21—C22	112.9 (7)
S6—C7—C6	113.2 (7)	S16—C22—C21	113.0 (9)

At 293 K, the structure shows disordered ethylenic groups as a result of the existence of two different sites with different energies (Williams, Wang, Emge, Geiser, Beno, Leung, Carlson, Thorn, Schultz & Whangbo, 1987).

In order to characterize those sites, we have performed an occupancy refinement on the ethylenic C-atom positions. This converges unambiguously towards two sites (Table 2a) for only one group of the *A* molecule (C11, C11', C12, C12'), the other being ordered (C6, C7) and for the two groups of the *B* molecule group (C16, C16', C17, C17', C21, C21',

C22, C22') (Fig. 1). In fact, such character is quite usual in the ET salts.

Upon cooling, only the *b* axis contracts while the *a* and *c* axes increase considerably in length, as does the  $\beta$  angle, to achieve their maximum at 200 K after which lattice contraction became normal (Fig. 3). This phenomenon has already been observed in this kind of salt (Schultz, Beno, Geiser, Wang, Kini, Williams & Whangbo, 1991), but not with such magnitude. This behaviour could be closely related to a kinetic mechanism of ordering. In addition to the interstack S...S interactions (Fig. 4), we note that

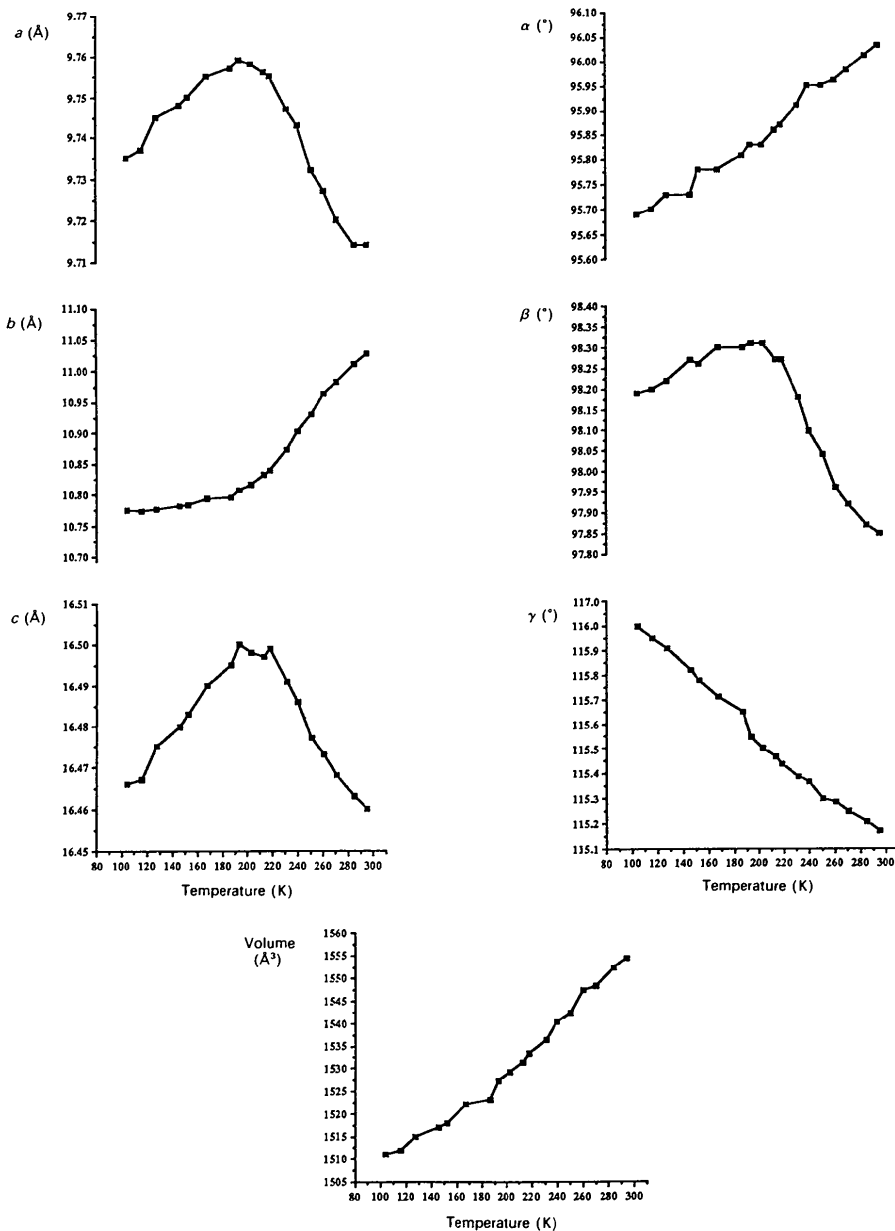
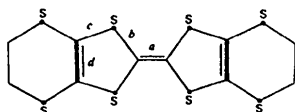


Fig. 3. Variation of the unit-cell parameters versus temperature.

Table 4. Comparison of the averaged intramolecular distances (Å) for various observed charges on the BEDT-TTF molecules



Temp.	Molecule	a	b	c	d	Ref.
—	ET <sup>0</sup>	1.319 (10)	1.757 (10)	1.753 (10)	1.331 (10)	(1)
—	ET <sup>1/2+</sup>	1.360 (10)	1.732 (9)	1.744 (9)	1.340 (10)	(2)
—	ET <sup>+</sup>	1.388 (10)	1.720 (11)	1.737 (10)	1.345 (15)	(3)
293 K	A	1.364 (7)	1.732 (5)	1.744 (5)	1.344 (7)	(4)
	B	1.349 (7)	1.737 (5)	1.744 (5)	1.335 (7)	(4)
135 K	A	1.36 (1)	1.73 (1)	1.74 (1)	1.31 (1)	(4)
	B	1.35 (1)	1.744 (9)	1.750 (9)	1.34 (1)	(4)
293 K	A	1.363 (4)	1.730 (3)	1.743 (4)	1.348 (4)	This work
	B	1.364 (4)	1.732 (3)	1.742 (3)	1.345 (5)	—
100 K	A	1.34 (2)	1.75 (1)	1.75 (1)	1.34 (2)	—
	B	1.32 (1)	1.76 (1)	1.742 (3)	1.345 (5)	—

References: (1) Kobayashi *et al.* (1986); (2) Mallah *et al.* (1990); (3) Triki *et al.* (1991); (4) Fettouhi *et al.* (1992).

the ET molecules lay nearly parallel to the (010) face, and give rise to short metal–hydrogen contacts as found in the corresponding Pt salts (Fettouhi *et al.*, 1992). Therefore, taking into account the ethylenic environment, the order–disorder transition requires a geometrical rearrangement to achieve sites of lowest energy and because of the ET orientation the parameters influenced most are *a*, *c* and  $\beta$ , respectively (Figs. 3, 4).

At 100 K, the structure is not significantly different to that observed at 293 K. We note that the intrastack distances are not considerably altered and remain greater than 3.8 Å. In contrast the most important contraction gives strong interactions between molecules of adjacent stacks with S...S distances in the range of 3.322 (5)–3.678 (5) Å (Table 5, Fig. 5). This behaviour is quite common in quasi-two-dimensional salts. Moreover, the terminal ethyl-

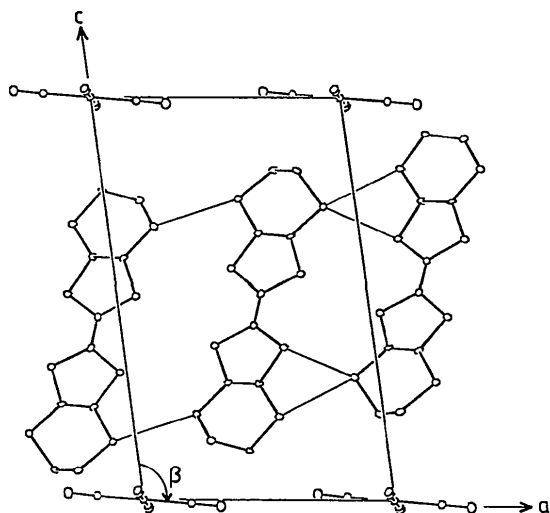


Fig. 4. Projection down the *b* axis showing that the most important contacts occur in the (010) plane.

Table 5. Comparative intermolecular interactions (Å) at 293 and 100 K

E.s.d.'s on the last digit are 0.001 (0.005 for 100 K) for S...S, 0.005 (0.012) for Ni...C, 0.006 (0.018) for C...N and 0.003 (0.012) for N...S.

Interstack interaction*	293 K		100 K		Anion–cation contacts	
	293 K	100 K	293 K	100 K	293 K	100 K
S2—S13 <sup>ii</sup>	3.372	3.322	Ni—C16 <sup>vi, vii</sup>	3.612	3.616	
S3—S14 <sup>viii</sup>	3.656	3.616	Ni—C17 <sup>vi, vii</sup>	3.472	3.700	
S4—S8 <sup>vii</sup>	3.591	3.678	N1—C7 <sup>v</sup>	3.458	3.479	
S5—S10 <sup>ii</sup>	3.506	3.411	N1—C21 <sup>v</sup>	3.357	3.481	
S5—S16 <sup>ii</sup>	3.404	3.403	N1—S15 <sup>v</sup>	3.652	3.514	
S6—S8 <sup>vii</sup>	3.453	3.455	N2—C7 <sup>v</sup>	3.383	3.310	
S7—S13 <sup>ii</sup>	3.340	3.347	N2—C22 <sup>vi</sup>	3.183	3.254	
S7—S15 <sup>viii</sup>	3.711	3.553	N2—S6 <sup>v</sup>	3.240	3.196	
S8—S10 <sup>ii</sup>	3.592	3.494	N2—S16 <sup>vi</sup>	3.361	3.334	
S9—S14 <sup>viii</sup>	3.496	3.452				
S14—S15 <sup>viii</sup>	3.433	3.461				

Symmetry code: (i) *x*, *y*, *z*; (ii)  $-1+x$ , *y*, *z*; (iii)  $-1+x$ ,  $-1+y$ , *z*; (iv)  $-1+x$ ,  $-1+y$ ,  $-1+z$ ; (v)  $-x$ ,  $1-y$ ,  $-z$ ; (vi)  $1-x$ ,  $1-y$ ,  $-z$ ; (vii)  $1-x$ ,  $1-y$ ,  $1-z$ ; (viii)  $1-x$ ,  $2-y$ ,  $1-z$ .

\*The intrastack S...S distances are greater than the sum of the van der Waals radii.

enic groups become ordered and when viewed along the central C—C double bond, the two groups are staggered relative to each other as shown in Fig. 1. The distances (Å) to the mean plane of the central TTF units for the terminal C atoms are: C6, 0.702 (12); C7,  $-0.021$  (12); C11,  $-0.286$  (13); C12, 0.446 (14); C16,  $-0.386$  (13); C17, 0.344 (15); C21, 0.092 (13); C22, 0.904 (14).

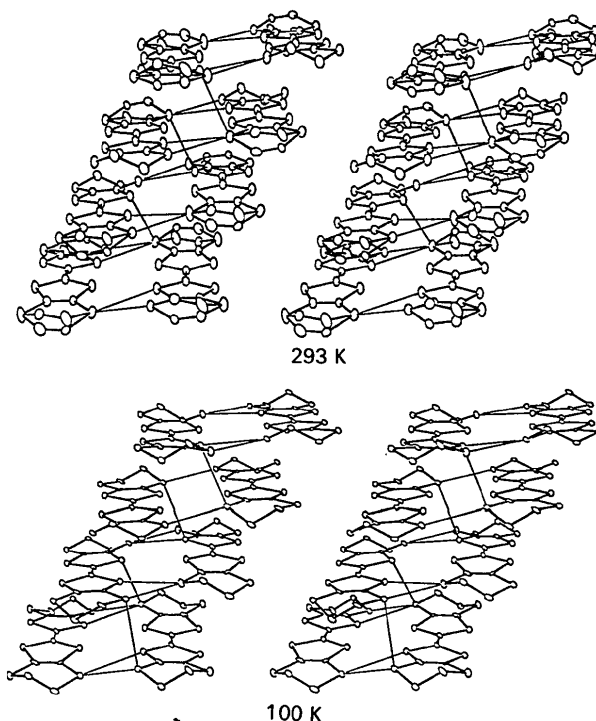


Fig. 5. Stereoscopic view of the ET packing at both 293 and 100 K. The interstack S...S contacts  $\leq 3.65$  Å according to Table 5 are drawn.

A stereoscopic view of the packing of the ET molecules is presented in Fig. 5. This arrangement is of the  $\beta$ -type (Williams *et al.*, 1987). As commonly observed in the quasi-two-dimensional type of compounds the most significant intermolecular S...S contacts are established between adjacent stacks.

#### References

- B. A. FRENZ & ASSOCIATES INC. (1985). *SDP Structure Determination Package*. College Station, Texas, USA, and Enraf-Nonius, Delft, The Netherlands.
- BENCHARIF, M. & OUAHAB, L. (1988). *Acta Cryst.* **C44**, 1514–1516.
- Enraf-Nonius (1985). *CAD-4 Program*. Version 4.1. Enraf-Nonius, Delft, The Netherlands.
- FETTOUHI, M., OUAHAB, L., GRANDJEAN, D. & TOUPET, L. (1992). *Acta Cryst.* **B48**, 275–280.
- GARRIGOU-LAGRANGE, C., OUAHAB, L., GRANDJEAN, D. & DELHAES, P. (1990). *Synth. Met.* **35**, 9–16.
- KAWAMOTO, A., TANAKA, M. & TANAKA, J. (1991). *Bull. Chem. Soc. Jpn.* **64**, 3160–3162.
- KOBAYASHI, H., KOBAYASHI, A., SASAKI, Y., SAÏTO, G. & INOKUCHI, H. (1986). *Bull. Chem. Soc. Jpn.* **59**, 301–302.
- MALLAH, T., HOLLIS, C., BOTT, S., KURMOO, M., DAY, P., ALLAN, M. & FRIEND, R. H. (1990). *J. Chem. Soc. Dalton Trans.* **3**, 859–865.
- OUAHAB, L., PADIOU, J., GRANDJEAN, D., GARRIGOU-LAGRANGE, C., DELHAES, P. & BENCHARIF, M. (1989). *J. Chem. Soc. Chem. Commun.* pp. 1038–1041.
- OUAHAB, L., TRIKI, S., GRANDJEAN, D., BENCHARIF, M., GARRIGOU-LAGRANGE, C. & DELHAES, P. (1990). *Lower-Dimensional Systems and Molecular Electronics*, Vol. 284, edited by R. M. METZGER, pp. 185–190. New York. Plenum Press.
- SCHULTZ, A. J., BENO, M. A., GEISER, U., WANG, H. H., KINI, A. M., WILLIAMS, J. M. & WHANGBO, M. H. (1991). *J. Solid State Chem.* **94**, 352–361.
- TRIKI, S., OUAHAB, L., GRANDJEAN, D. & FABRE, J. M. (1991). *Acta Cryst.* **C47**, 645–648.
- WALKER, N. & STUART, D. (1983). *Acta Cryst.* **A39**, 158–166.
- WILLIAMS, J. M., WANG, H. H., EMGE T. J., GEISER, U., BENO, M. A., LEUNG, P. C. W., CARLSON, K. D., THORN, R. J., SCHULTZ A. J. & WHANGBO, M. H. (1987). *Prog. Inorg. Chem.* **35**, 51–218.

*Acta Cryst.* (1993). **B49**, 691–698

## X-ray Diffraction Study of the Ferroelectric Phase Transition of $(\text{CH}_3)_4\text{NCdBr}_3$ (TMCB)

BY G. AGUIRRE-ZAMALLOA

*Laboratoire de Spectroscopie Moléculaire et Cristalline, URA 124, CNRS, Université de Bordeaux I, 33405 Talence CEDEX, France*

G. MADARIAGA

*Departamento de Física de la Materia Condensada, Facultad de Ciencias, Universidad del País Vasco, Apdo. 644, 48080 Bilbao, Spain*

M. COUZI

*Laboratoire de Spectroscopie Moléculaire et Cristalline, URA 124, CNRS, Université de Bordeaux I, 33405 Talence CEDEX, France*

AND T. BRECZEWSKI

*Departamento de Física Aplicada II, Facultad de Ciencias, Universidad del País Vasco, Apdo. 644, 48080 Bilbao, Spain*

(Received 20 November 1992; accepted 16 February 1993)

#### Abstract

The crystal structure of tetramethylammonium tribromocadmiate (II),  $[\text{N}(\text{CH}_3)_4][\text{CdBr}_3]$  (TMCB), has been studied at 295 and 85 K, in order to analyze the structural changes connected with the improper para-ferroelectric phase transition occurring at  $\sim 160$  K. The space group of the paraelectric (room-temperature) phase is  $P6_3/m$  and that of the ferroelectric (low-temperature) phase is  $P6_1-P6_5$ . Final

agreement factors are  $R(wR) = 0.062$  (0.075) and  $R(wR) = 0.029$  (0.038) for the data collected at 295 and 85 K respectively. It is shown that this phase transition is related to an orientational order-disorder process of the tetramethylammonium (TMA) groups, which leads to a tripling of the lattice constant along the  $c$  (hexad) direction; this process can be described by the freezing of a pseudo-spin coordinate defined in the frame of a Frenkel-type model. In addition, the helical-type structure found for the ferroelectric